[18]P. G. Klemens, Proc. Phys. Soc. (London) A68, 1113 (1955).
[19]C. Herring, Phys. Rev. 95, 954 (1954).
[20]P. G. Klemens, in *Solid State Physics*, edited by F. Seitz and D. Turnbull (Academic, New York, 1968), Vol. 7, p. 1.
[21]J. R. D. Copley, R. W. Macpherson, and T. Timusk, Phys. Rev. 182, 965 (1969).
[22]G. Raunio and S. Rolandson, Phys. Rev. B 2, 2098 (1970).
[23]C. T. Walker and R. O. Pohl, Phys. Rev. 131, 1433 (1963).
[24]J. M. Worlock, Ph.D. thesis (Cornell University, 1962) (unpublished).

PHYSICAL REVIEW B VOLUME 6, NUMBER 10 15 NOVEMBER 1972

Convergence of Reciprocal-Lattice Expansions and Self-Consistent Energy Bands of NaF†

N. E. Brener
Department of Physics and Astronomy, Louisiana State University, Baton Rouge, Louisiana 70803
and
J. L. Fry
Department of Physics, University of Texas, Arlington, Texas 76010
(Received 13 January 1972)

A convergence study is made of the reciprocal-lattice expansion of linear-combination-of-atomic-orbitals integrals in NaF. Converged integrals are obtained by direct summation and by extrapolation after different numbers of terms. It is found that extrapolation procedures give simple accurate results and substantially reduce labor involved. Comparison is made with other methods for obtaining convergence. Converged integrals are used as a basis for a self-consistent Hartree–Fock–Slater energy-band calculation for NaF using methods previously developed. Some transition energies are presented and correlated with available optical data. Self-consistent charge densities in NaF differ only slightly from a linear combination of ionic charge densities, confirming the ionic nature of NaF.

I. INTRODUCTION

The linear-combination-of-atomic-orbitals (LCAO) method which was first proposed[1] in 1928 has only recently been developed to its full power.[2–11] While there are still some theoretical questions of its applicability to quantitative solid-state calculations, practical experience indicates that it not only is as accurate as other methods when done correctly, but also has great advantage in self-consistent calculations[5] or problems involving Brillouin-zone sampling or computation of matrix elements using Bloch wave functions. However, when reading the literature of LCAO or tight-binding calculations one must be careful to distinguish between approximate LCAO calculations and ones which are performed with new techniques. Neglect or approximation of multicenter integrals and inclusion of only limited numbers of neighbors usually means that the energy bands are qualitative at best. Discussions of the problems encountered in accurate LCAO procedures are given in Refs. 6, 11, and 12.

In this paper special attention is paid to convergence properties of the reciprocal-lattice series expansion of LCAO integrals. Some of the methods used to facilitate summation of these series are discussed in Sec. II. In Sec. III, well-converged integrals for NaF are used to perform a self-consistent Hartree–Fock–Slater energy-band calculation.

II. CONVERGENCE OF LCAO INTEGRALS

The LCAO method employed here has been discussed elsewhere[2,3,7] and will not be presented again. Accuracy in LCAO energy bands requires a critical analysis of all approximations made. In this section attention is focused upon convergence of reciprocal-lattice expansions of various LCAO integrals.

Reciprocal-lattice sums are a result of expressing the crystal potential as a Fourier series in order to circumvent calculation of three-center integrals. Approximation or complete neglect of the difficult three-center integrals and failure to sum enough direct-lattice neighbors invalidated early efforts to use the LCAO method in first-principles calculations. The Fourier-series technique permits accurate evaluation of LCAO integrals and produces accurate energy bands.

Introduction of Gaussian orbitals instead of Slater (exponential) orbitals greatly simplifies and

accelerates the numerical work. Use of the Fourier series for the crystal potential and use of Gaussian basis functions for the atomic orbitals yield analytic expression for all matrix elements needed in evaluation of the LCAO secular determinant. However, the rate of convergence of the reciprocal-lattice sums for some LCAO integrals may be very slow, making it difficult to estimate the error after a given number of terms. In some instances convergence is so slow that it is essential to find ways of accelerating it in order to obtain the necessary accuracy in reasonable computer times. Examples of the sort of errors which may occur with inadequate convergence are given in Ref. 12.

A typical LCAO integral is expressed as

$$\int \phi_i(\vec{r})\, V(\vec{r})\, \phi_j(\vec{r}-\vec{R}_l)\, d^3r$$

$$= \sum_{K_n} V(\vec{K}_n) \int \phi_i(\vec{r})\, e^{i\vec{K}_n\cdot\vec{r}}\, \phi_j(\vec{r}-\vec{R}_l)\, d^3r$$

$$\equiv \sum_{K_n'} V(\vec{K}_n)\, E_{ij}(\vec{K}_n, \vec{R}_l)\ ,$$

where ϕ_i and ϕ_j are orbitals of given symmetries centered at the origin and at site $\vec{R}_l$, respectively. The Gaussian atomic orbitals used for Na and F are given in Table I. $V(\vec{r})$ is the periodic crystalline potential and $V(\vec{K}_n)$ is its Fourier transform. The starting (first-iteration) crystal potential was constructed as a linear superposition of ionic potentials as discussed in previous publications.[7,12]

Convergence of the reciprocal-lattice sum is governed by both $V(\vec{K}_n)$ and the integral $E_{ij}(\vec{K}_n, \vec{R}_l)$. The latter will depend upon the symmetry of orbitals involved, values of the orbitals exponents, separation of the orbitals, $\vec{R}_l$, and the value of $\vec{K}_n$. At large $\vec{K}_n$ the dominant contribution to $V(\vec{K}_n)$ comes from the nuclear point charge

$$V(\vec{K}_n) \to -4\pi Z e^2/K_n^2\ .$$

For large $\vec{K}_n$ the integral $E_{ij}(\vec{K}_n, \vec{R}_l)$ is more complicated, depending upon types of orbitals involved, but all types include a factor $\exp[-\vec{K}_n^2/4(\alpha_1+\alpha_2)]$, where α_1 and α_2 are exponents in the Gaussian orbitals ϕ_i and ϕ_j. For large $\alpha_1+\alpha_2$ the $\vec{K}_n$ dependence of $E_{ij}(\vec{K}_n, \vec{R}_l)$ is weak, and the rate of convergence is determined primarily by $V(\vec{K}_n)$ until $\vec{K}_n^2 > 4(\alpha_1+\alpha_2)$. $V(\vec{K}_n)$ gives very slow convergence, and it is mainly this term which must be overcome. For some combinations of symmetry and

TABLE I. Gaussian orbitals for sodium and fluorine. The s and p orbitals were obtained from Huzinaga and Sakai,[a] and d orbitals were generated by a Hartree-Fock calculation.

Sodium wave functions						Fluorine wave functions			
Orbital exponents of Gaussian basis set									
s		p		d		s		p	
1s	36631.1	2p	148.928	3d	6.000 00	1s	23342.2	2p	65.659 3
1s	5385.07	2p	34.514 9	3d	1.452 00	1s	3431.25	2p	15.218 7
1s	1216.20	2p	10.604 5	3d	0.102 959	1s	757.667	2p	4.788 19
1s	339.529	2p	3.671 06	3d	0.027 170	1s	209.192	2p	1.727 55
1s	109.563	2p	1.284 90	3d	0.009 342	1s	66.726 1	2p	0.648 123
1s	38.783 4	2p	0.430 941			1s	23.370 5	2p	0.244 965
1s	14.579 0	2p	0.166 490			1s	8.623 72	2p	0.091 537
1s	5.279 01	2p	0.051 793			1s	2.700 01		
1s	1.829 02	2p	0.018 420			1s	1.087 50		
1s	0.620 535					1s	0.396 536		
1s	0.058 065					1s	0.172 324		
1s	0.024 617								

Orbital expansion coefficients of Gaussian basis set

1s	2s	3s	2p	3p	3d	1s	2s	2p
0.000 38	−0.000 09	0.000 01	0.005 147	−0.000 511	0.000 166	0.000 40	−0.000 09	0.008 82
0.003 05	−0.000 74	0.000 11	0.037 920	−0.003 805	0.002 705	0.003 27	−0.000 75	0.057 78
0.015 99	−0.003 96	0.000 60	0.153 743	−0.015 526	0.069 251	0.017 54	−0.004 09	0.193 41
0.064 27	−0.016 13	0.002 41	0.352 821	−0.036 470	0.451 313	0.070 82	−0.016 99	0.356 71
0.194 81	−0.053 10	0.008 22	0.457 887	−0.047 405	0.630 163	0.212 90	−0.054 76	0.392 96
0.400 99	−0.127 76	0.019 15	0.239 507	−0.040 177		0.422 13	−0.131 95	0.229 90
0.392 67	−0.199 52	0.033 11	−0.000 105	0.070 060		0.374 80	−0.184 73	0.031 43
0.082 82	0.034 27	−0.010 52	0.006 753	0.494 273		0.058 66	0.081 75	
−0.002 65	0.598 03	−0.098 98	−0.002 405	0.551 837		−0.009 44	0.551 15	
0.001 77	0.485 79	−0.206 86				0.004 68	0.445 02	
−0.000 31	0.016 63	0.599 48				−0.001 36	0.061 82	
0.000 17	−0.007 62	0.484 01						

[a] S. Huzinaga and Y. Sakai, J. Chem. Phys. 50, 1371 (1969).

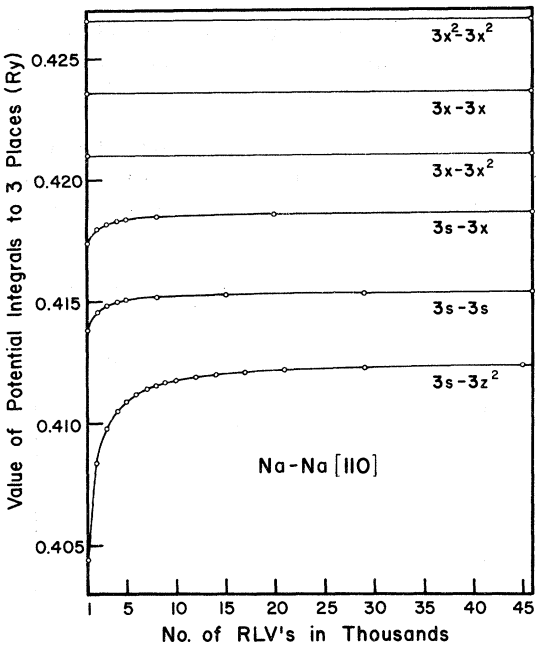

FIG. 1. Convergence behavior of reciprocal-lattice sums for various Na-Na first-neighbor integrals. The integrals were computed in rydbergs, but arbitrary constant shifts have been made to display them on the same graph. $3x$ is a $3p$ function transforming like x, while $3x^2$ and $3z^2$ are $3d$ functions transforming like x^2-y^2 and $3z^2-r^2$, respectively.

α_1 and α_2 the $\vec{K}_n$ dependence of $E_{ij}(\vec{K}_n, \vec{R}_l)$ is strong enough to produce rapid convergence in spite of $V(\vec{K}_n)$, but this is only occasionally the case, e.g., d-d integrals encountered in this paper. While a simple analytic expression for the nth term in the reciprocal-lattice sum may be written down for a single s-like Gaussian orbital, the atomic orbitals, which are linear combinations of Gaussian orbitals, are more easily understood graphically.

Figure 1 shows the convergence behavior of different symmetry-type integrals as a function of the number of stars of reciprocal-lattice vectors summed. The integrals have been shifted by arbitrary constant amounts to be displayed on the same graph. While all have converged to three significant figures, some have converged to considerably more. Integrals shown are Na-Na first-neighbor values, but similar results are obtained for F-F- and NaF-type integrals. The problems occur with $3s$-$3p$ and $3s$-$3d$ symmetries. Core-core integrals are even more slowly convergent, but the only important ones are central-cell (two-center) integrals which may be handled without difficulty.

Figure 2 shows the behavior as a function of $\vec{R}_l$. Once again the integrals have been shifted by constant amounts. Note the significant figures indicating different degrees of convergence for different integrals. As separation of orbital sites becomes greater the rate of convergence increases, but only slightly in most cases. Convergence to fewer significant figures than indicated may be obtained more readily for larger $\vec{R}_l$.

The degree of localization of the orbitals also determines the rate of convergence. For Gaussian integrals this is indicated by the orbital exponents, larger parameters corresponding to greater localization. If atomic wave functions are used, as here, localization is roughly indicated by the principle quantum numbers of the atomic orbitals. Figure 3 shows these trends for some of the integrals which are slowly convergent.

The slowness of convergence for some of the integrals shown in Figs. 1–3 can be appreciated fully by reference to Table II, where selected integrals are given at different stages of summation. In order to gain understanding of these convergence properties the authors attempted to perform an analysis similar to the methods used by Euwema and Stukel to study orthogonalized-plane-wave (OPW) convergence in tetrahedral semiconductors. [13] Their work is of great pedagogical as well as practical value and is recommended reading for anyone interested in band theory.

Attempts which were made here to perform a similar study met with immediate failure. In the LCAO method the Fourier-series expansion is made for the potential (rapidly varying near the origin), not the wave function (well-behaved near the origin). Also, the variational theorem is not working on the coefficients of expansion of the potential as it is in the case of the OPW expansion of the wave function. As a result it is necessary to sum terms to much larger K_{max}, corresponding to much smaller R_m, as defined in Ref. 13. The dominant potential term is the Coulomb potential of the nucleus, which is singular at the origin. Thus, convergence of LCAO Fourier-series expansion is more similar to the classic Ewald problem, as has already been pointed out. [3] The large number of terms necessary for convergence as indicated in Table II makes it clear that methods of accelerating convergence must be found if computer times are to remain reasonable.

Three different techniques have been used to obtain convergence: (i) an Ewald-type method, [3] (ii) integration, [10] and (iii) extrapolation. The Ewald method is described in Ref. 3. It uses an arbitrary auxilary potential function which falls rapidly to zero over a distance comparable to the lattice constant, but behaves near the nucleus like a point negative charge equal in magnitude to the nuclear charge. The Fourier transform of this function cancels the ill-behaved term in the Fourier trans-

form of the crystal potential for large $\vec{K}_n$. On the other hand, the short-range nature of the auxilary function permits approximation of its integral by one- or two-center terms, so that the part added to the Fourier series is subtracted out afterwards by direct integration. This method works only if the errors made in the two-center approximation to the auxilary potential integrals is valid for the particular orbitals and auxilary function used. It may be quite accurate if care is taken with the direct integral.[3]

The technique of integration consists of summing the Fourier series to some maximum $\vec{K}_n$ and approximating the sum of the remaining terms by

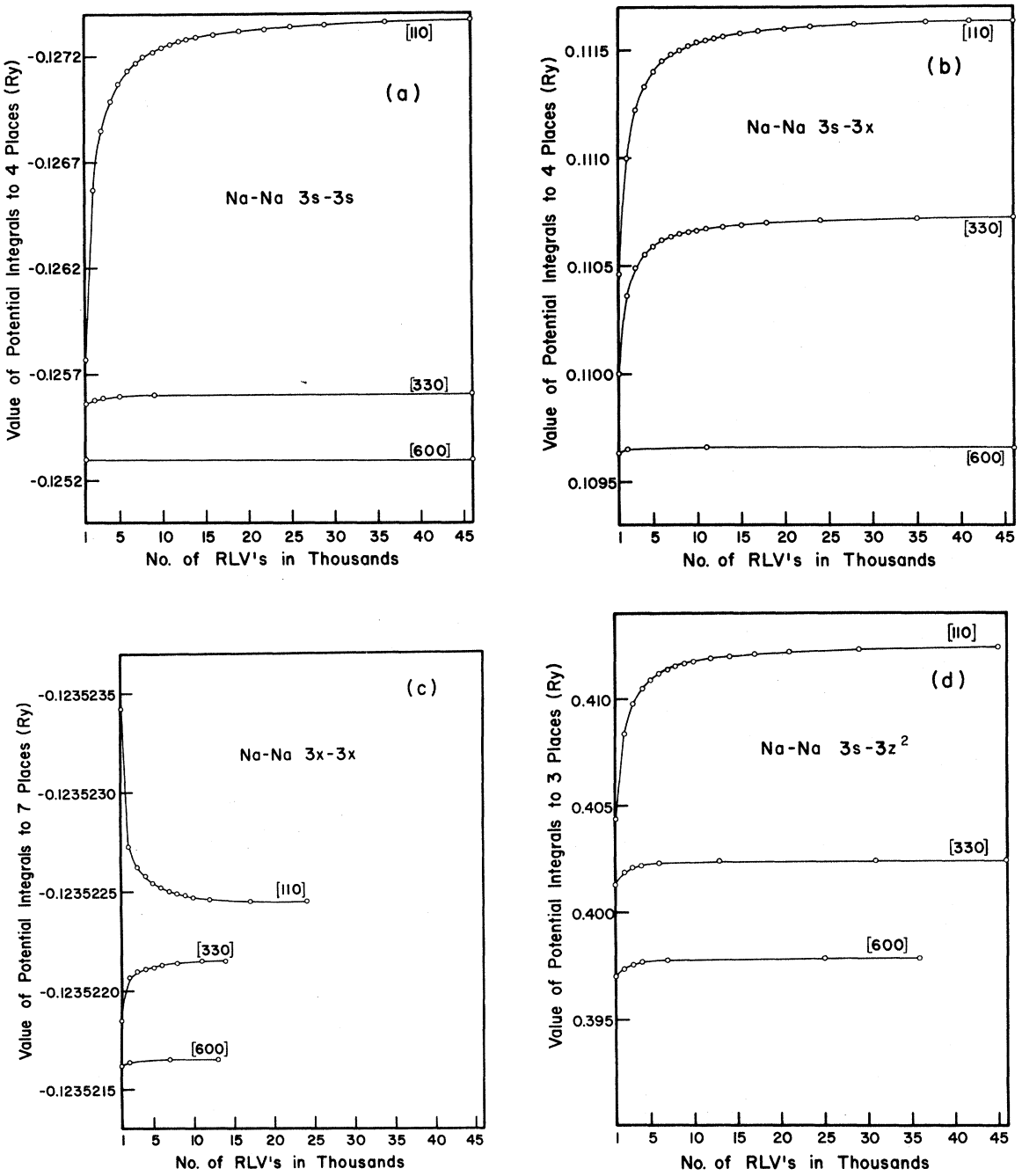

FIG. 2. Convergence behavior for different neighbors. Note the difference in scale indicating differences in convergence. The integrals have been shifted by arbitrary amounts.

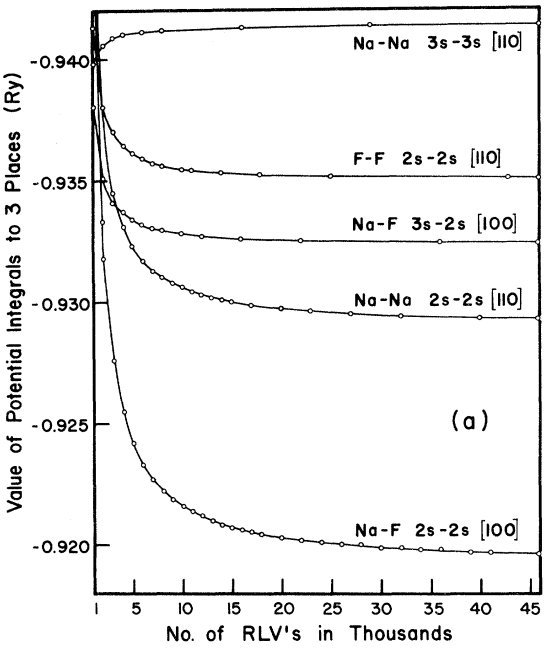

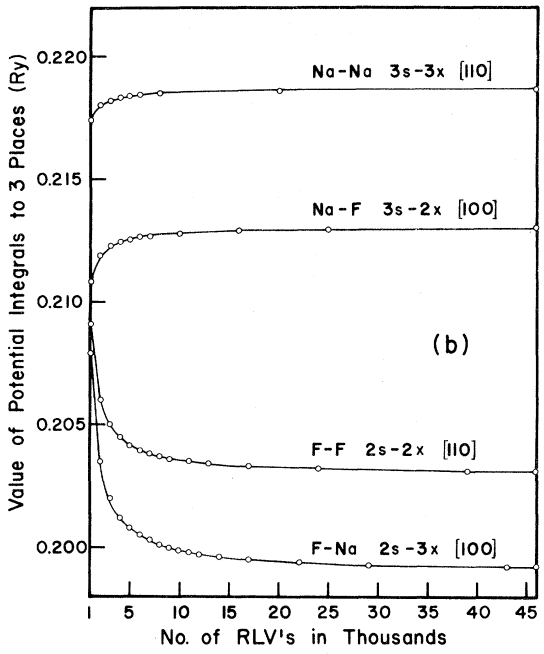

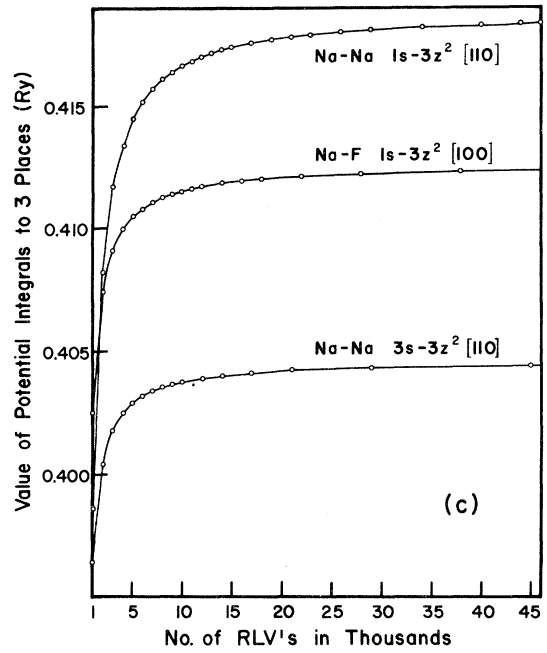

FIG. 3. Convergence behavior of various orbital types. The integrals have been shifted by arbitrary amounts.

converting the sum to an integral. Errors arise in this method from both the integration approximation and the numerical integration technique itself, but accurate answers may be obtained.

The technique of extrapolation can be the simplest of the three, depending upon the extrapolation procedure used. It should be possible to develop a Padé approximate to the series, but it would be different for each type of integral, and hence a substantial effort. A simple extrapolation method is obtained by observing that the sum after N stars is approximately a linear function of $1/N$, and an approximation to the converged value may be obtained by straight-line extrapolation to $1/N=0$ or $N=\infty$.

Figure 4 shows the asymptotic behavior of some of the integrals as a function of $1/N$. Figure 4(a) displays straight-line behavior in the region 1000 to 10 000 stars, while 4(b) shows the same integrals in the region to 47 000 stars. The slope is constant to more figures in Fig. 4(b), reflected by more significant figures in the extrapolated result. The values of various integrals obtained by extrapolating to $1/N=0$ after different numbers of reciprocal-lattice vectors (RLV) are shown in Table III. Even in the worst cases, extrapolation after summing 1000 RLV appears to be adequate for the accuracy needed in present-day band calculations. This represents a substantial savings in computer time, and further reductions would be realized with a nonlinear extrapolation procedure which would permit a smaller K_{max}.

III. SELF-CONSISTENT ENERGY BANDS

Self-consistent energy bands for NaF have been obtained using converged LCAO integrals as a basis. The self-consistent procedure used here has been discussed thoroughly elsewhere,[5,12] so it will not be elaborated again. Its simplicity rests upon the fact that it is not necessary to recompute (and

TABLE II. Convergence properties of some reciprocal-lattice sums for LCAO integrals. Integrals shown are all first-neighbor (110) Na-Na integrals. The last row shows estimated convergence after 47 000 stars. The last digit of the converged values is not expected to change upon further summation. $3z^2$ is a $3d$ function transforming like $3z^2-r^2$.

Stars (10^3)	$2s$-$2s$ (10^{-3}Ry)	$3s$-$3s$ (Ry)	$3s$-$3p_x$ (Ry)	$2s$-$3z^2$ (Ry)	$3s$-$3z^2$ (Ry)
1	−0.588 304	−0.125 768	0.110 359	0.160 352	0.040 444
5	−0.575 256	−0.127 074	0.111 401	0.156 095	0.041 093
10	−0.573 571	−0.127 241	0.111 534	0.155 546	0.041 176
20	−0.572 718	−0.127 324	0.111 601	0.155 268	0.041 217
30	−0.572 439	−0.127 352	0.111 623	0.155 178	0.041 231
40	−0.572 302	−0.127 365	0.111 634	0.155 134	0.041 238
	−0.572	−0.127 3	0.111 6	0.155	0.041 2

reconverge) LCAO integrals at each stage of iteration, but iterated matrix elements are expressed in terms of initial matrix elements. To simplify the self-consistent calculation, only the following

TABLE III. Extrapolated first-neighbor Na-Na integrals. Column 2 shows values obtained by extrapolating with slope determined by values after 1000 and 2000 stars, column 3 for 2000–5000, and column 4 for 5000 – 10 000 stars. The last column shows convergence estimated by extrapolating from 47 000 stars. All energies are in rydbergs.

Integral	1–2	2–5	5–10	Converged
$1s-3z^2$	0.417 783	0.418 666	0.418 813	0.418 8
$2s-3z^2$	0.155 124	0.155 000	0.154 997	0.154 999
$3s-3z^2$	0.412 419	0.412 594	0.412 583	0.412 406
$1s-2x$	−0.364 335	−0.364 148	−0.364 093	−0.364 09
$2s-2x$	0.308 940	0.308 998	0.308 994	0.309 002
$3s-2x$	0.282 079	0.282 133	0.282 130	0.282 137
$1s-3x$	0.670 637	0.672 053	0.672 289	0.672 3
$2s-3x$	0.251 493	0.251 294	0.251 289	0.251 29
$3s-3x$	0.111 661	0.111 641	0.111 669	0.111 666
$1s-1s$	−0.510 354	−0.511 438	−0.511 614	−0.511 6
$2s-1s$	−0.649 373	−0.650 742	−0.650 972	−0.651 0
$3s-1s$	−0.421 083	−0.421 972	−0.422 120	−0.422 2
$2s-2s$	−0.572 287	−0.571 897	−0.571 885	−0.571 89
$3s-2s$	−0.160 260	−0.160 136	−0.160 132	−0.160 134
$3s-3s$	−0.127 374	−0.127 409	−0.127 407	−0.127 406

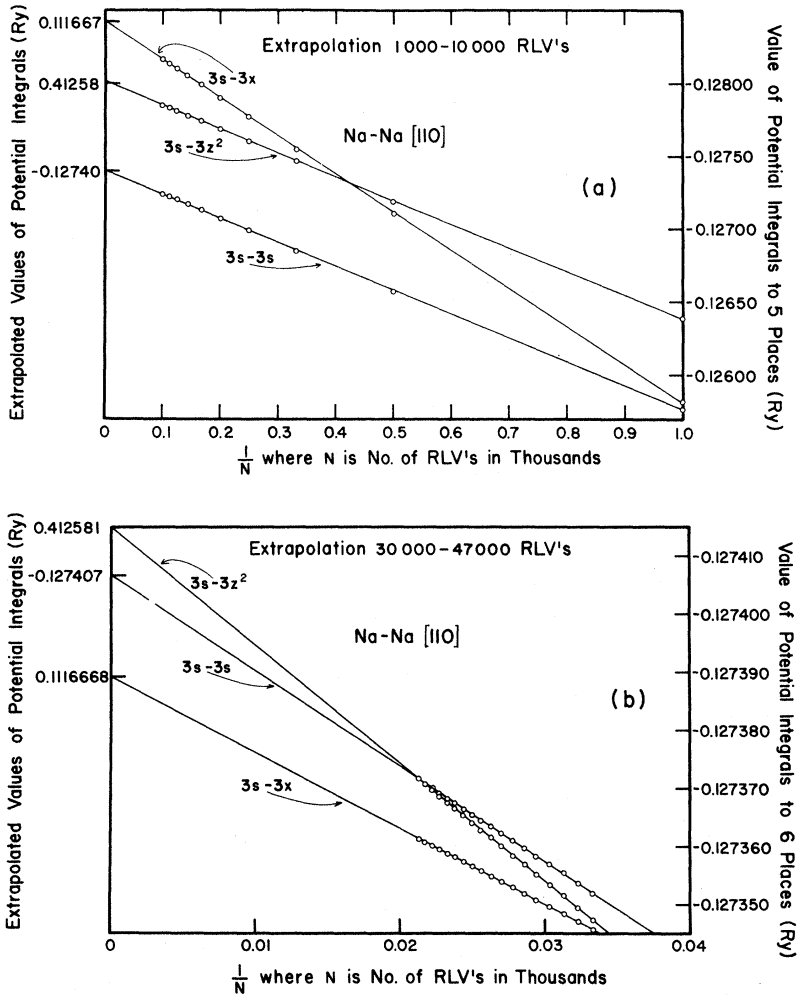

FIG. 4. Extrapolation of reciprocal-lattice sums. (a) shows extrapolation from the region of 1000–10 000 stars of RLV while (b) shows the region 30 000 to 47 000 stars of RLV. The scale to the right-hand side indicates the number of significant figures and the left-hand scale shows extrapolated values. Agreement between extrapolated values in (a) and (b) is good, one more significant figure being available from (b) (energy in rydbergs).

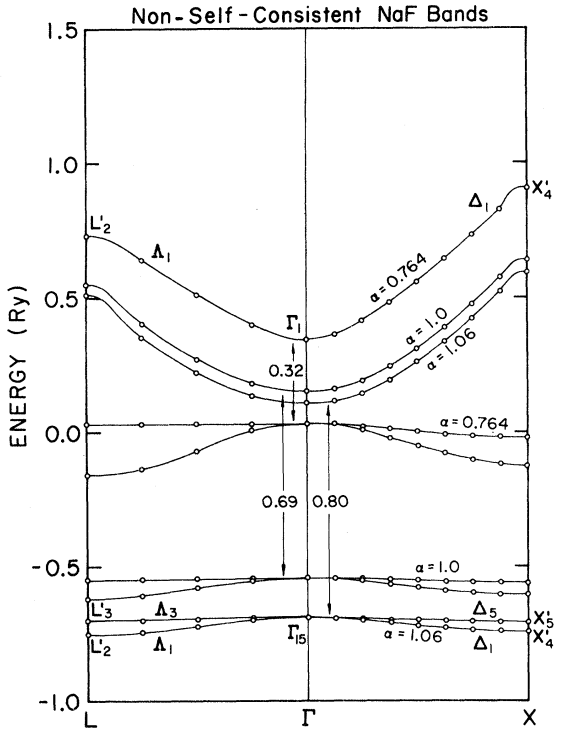

FIG. 5. Non-self-consistent NaF energy bands.

orbitals were included in the basis set:

Na: $1s$, $2s$, $3s$, $2p$, $3p$,

F: $1s$, $2s$, $2p$.

These orbitals lead to 14×14 Hamiltonian and overlap matrices. During self-consistent interations the Na $3s$ and $3p$ components played only a very minor role in determining the self-consistent potential. d-like orbitals are expected to play an even smaller role and were not included in the set. Other calculations[14] indicate that d-electron levels do lie fairly low in the conduction bands of alkali halides and must be included for an accurate description of optical transitions much above the fundamental absorption edge. For this purpose d functions may be added after the self-consistent potential has been obtained. Since they have not been included in this calculation only the lowest conduction band may be considered reliable at this point.

Energy bands obtained from the starting crystal potential are shown in Fig. 5. The lattice constant used was 4.62 Å. Three values of the X_α exchange parameter are shown: $\alpha = 1$ Slater exchange, $\alpha = 1.06$, and $\alpha = 0.764$. The immediate conclusion to be drawn from these bands is that it was not possible to find an exchange parameter in the range $\frac{2}{3} \leq \alpha \leq 1$ in a non-self-consistent band calculation to yield agreement with the measured gap[15,16] of 0.85 Ry. While this was not the experience with LiF, similar behavior occured for other alkali halides in the work of Page and Hygh.[14]

An integration grid consisting of 89 points in $\frac{1}{48}$ of the fcc Brillouin zone was used to obtain self-consistent charge densities and energy bands. Rearrangement of charge during the self-consistent iterations produced wider energy gaps for fixed α: Figure 6 shows self-consistent energy bands for $\alpha = 1.06$. The computed gap 0.84 Ry is in good agreement with the observed gap of about 0.85 Ry.[17] The valence bandwidth is 0.7 eV, which is comparable with the bandwidth obtained in LiF calculations,[12,14,18,19] but smaller than the value quoted by Gout *et al.*[20] of 3.44 eV. This latter value should not be regarded as quantitatively meaningful because of approximations made in constructing the crystal potential and also approximations in application of the tight-binding method. These approximations probably account for the off-center maximum of the valence band in Ref. 20. The minimum energy gaps obtained in all band calculations reported here were direct and occurred at the Γ point of the Brillouin zone.

Experimental data which may be compared with the band structures obtained here consist of the fundamental absorption edge,[15,16] photoemission measurements,[21] and extreme ultraviolet absorption.[22,23] Ultraviolet transmission or reflection

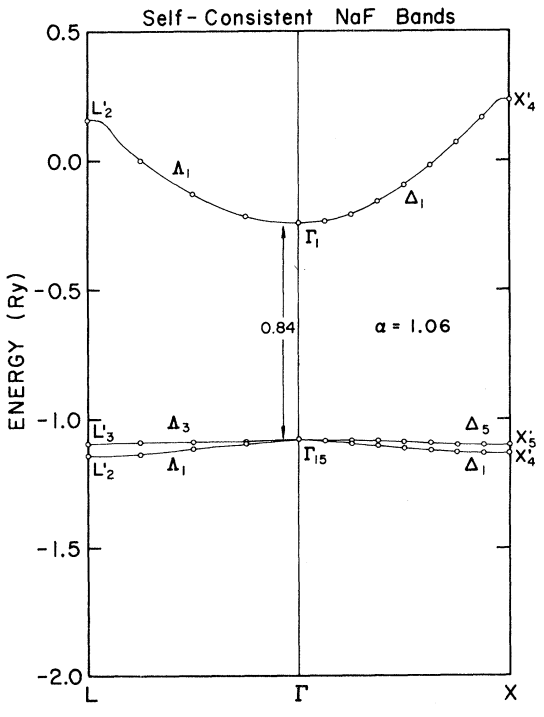

FIG. 6. Self-consistent NaF bands without polarization corrections.

experiments[24] above 12 eV are limited by the transmission of LiF windows conventionally used on low-temperature vacuum sample holders, so only a small portion of the optical spectrum of NaF above the fundamental absorption edge has been measured. While the usual exciton is clearly evident in the data, location of the fundamental absorption edge is somewhat uncertain because it falls in, or near, the region of absorption by the LiF excitons, and absorption by the LiF windows becomes large. The fundamental absorption edge is estimated to be about 11.5 eV for NaF. The photoemission edge has been found to be about 10–12 eV in the work of Duckett and Metzger.[21]

Extreme ultraviolet spectra has been obtained[22] using synchrotron-radiation sources, and an initial attempt to analyze such data has been made by Brown *et al.*[23] Transitions arising from the $2p$ levels of the sodium ion have been tabulated by Haensel *et al.*[22] and may be correlated with the fundamental absorption. Assuming the first two peaks in the NaF spectra (labeled A and B in Ref. 22) correspond to excitons, the absorption edge may be estimated. A numerical value for the absorption edge is not given in Ref. 22, but inspection of the spectrum suggests that it is approximately 34 eV for the transition $\mathrm{Na}(2p) \rightarrow \Gamma_1$.

The following comparisons may be made between theory and experiment: (i) The fundamental absorption edge could be fit; (ii) the computed absorption edge for the $\mathrm{Na}(2p)$ transitions was 33.3 eV compared to 34.0 eV from experiment; and (iii) the photoemission edge was computed to be 14.7 eV compared to 10–12 eV.

The position of the $\mathrm{Na}(2p)$ absorption edge depends strongly upon the exchange potential, even more than the fundamental edge, and better agreement with this edge could be obtained when α was not constrained to give exactly the fundamental edge. A similar result was obtained in LiF: For $\alpha = 0.87$ an exact fit occurred to the fundamental gap, but the $\mathrm{Li}(1s)$ edge was missed by 5 eV. A slightly larger α gave reasonable agreement for both edges. Failure to gain exact agreement for both gaps when fitting one of them probably reflects inadequacy of the local-exchange-potential approximation. This conclusion need not be drawn at this time, however, as polarization corrections to the bands have not been computed nor is the experimental data, particularly assignment of edge positions, all that certain.

In Table IV some of the calculated transitions ($\alpha = 1.06$) are compared with the data of Ref. 22. There appears to be some correlation between theoretical values of transition energies from the top valence band (L_3' and X_5') to the conduction band and the extreme ultraviolet absorption peaks given by Haensel *et al.*[22] Since the top valence band is very narrow, the peak structure due to these transitions should resemble the spectra observed from the narrow $\mathrm{Na}(2p)$ bands. However, it is not possible to make definite assignments without a complete calculation of $\epsilon_2(\omega)$. While it is tempting to assign peaks to symmetry points in the Brillouin zone, it has been found by detailed calculation[25] that this is not reliable, since peak structures usually arise from oscillator contributions throughout the zone and, e.g., transitions which are dipole forbidden at symmetry points may appear as a result. Extreme ultraviolet data is especially hard to analyze because it represents many possible interband transitions from different sets of bands with the same energy separations. Possible contributions in the 34-eV range for NaF are $\mathrm{Na}(2p)$ to low conduction bands and $\mathrm{F}(2s)$ to low conduction bands as well as transitions from the upper valence band to higher conduction bands. A further complication in identifying the structure is the assignment of exciton peaks. The peaks labeled A and B in the data of Haensel *et al.* fall at the same position in all the sodium halides and are tentatively identified by them as exciton peaks. Brown *et al.*[23] question whether any of the extreme ultraviolet structure may be identified as exciton peaks with any certainty, but Fong and Cohen[25] assign peaks A, B, and C to excitons in their $\epsilon_2(\omega)$ studies for NaCl.

IV. CONCLUSION

In Sec. III it was demonstrated that the converged LCAO integrals provided an adequate basis for self-consistent Hartree–Fock–Slater energy-band calculations. Using the same techniques as in the LiF calculation it was possible to obtain reasonable agreement with several pieces of experimental data. A complete analysis of the extreme ultraviolet absorption data for NaF requires the inclu-

TABLE IV. Comparison of computed fundamental-absorption energies with measured extreme ultraviolet absorption. Column 1 lables the fundamental transitions and column 4 shows tentative assignments of terminal levels of the extreme ultraviolet transitions from the $\mathrm{Na}(2p)$ band. All energies are in rydbergs. The labels of column 7 were given in Ref. 22. The peak labeled C may be an exciton, as concluded in Ref. 25.

	Calculated		Experiment: Na($2p$)		
$F(2p)$	Energy	ΔE	Energy	ΔE	Label
$\Gamma_{15} \rightarrow \Gamma_1$	11.4	0	34.0	0.0	···
			35.5	1.5	C
$L_3' \rightarrow L_2'$	17.0	5.6	39.2	5.2	D
$L_3' \rightarrow L_1$	17.2	5.8			
$X_5' \rightarrow X_4'$	18.1	6.7	41.6	7.6	E
$X_5' \rightarrow X_1$	20.0	8.6	46.3	12.3	F

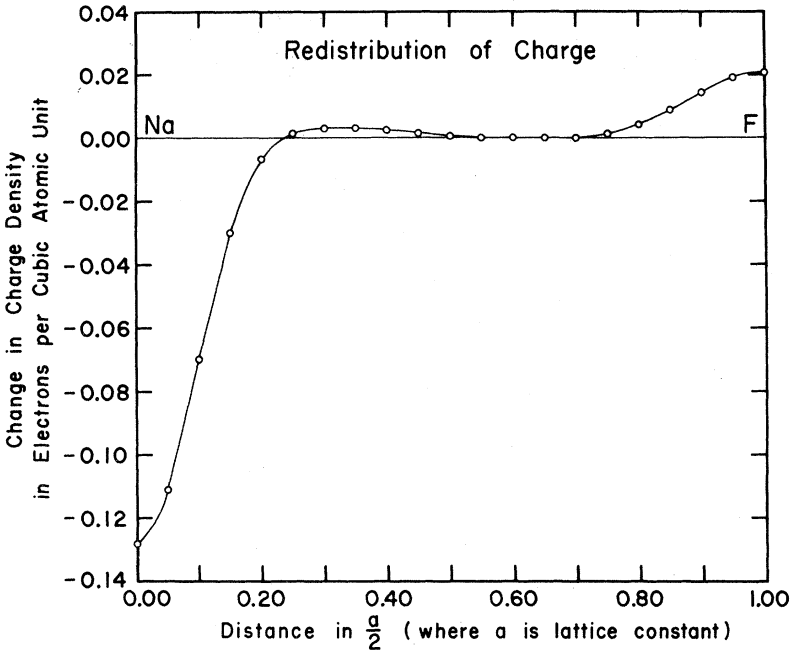

FIG. 7. Change in charge density along the [100] axis produced by self-consistency. Similar changes occur along other axes.

sion of d-like conduction bands and a complete calculation of $\epsilon_2(\omega)$. This will be the subject of a future work.

Before concluding, a few observations about the self-consistent charge distribution of NaF should be made. The starting potential was constructed from ionic charge distributions for Na^+ and F^-. Charge redistribution which occurred in the self-consistent calculation for NaF is shown in Fig. 7. A net movement of electrons from the fluorine ion to the sodium ion has occurred. An approximate value for the amount of charge moved was obtained by performing a volume integral from the ions out to the points where the charge density went through zero. About 0.06 electron was removed from the fluorine ion and 0.09 was placed upon the sodium ion. The rest of the negative charge placed on the sodium ion came from the interstitial regions. The total amount of valence charge redistributed was about 0.09 electron, so that the change in charge density of the valence electrons from the ionic to the self-consistent configuration was less than 10%, and therefore NaF is at least 90% ionic. This is in agreement with the LiF results of Drost and Fry.[12]

Simple binding-energy calculations,[26] based upon an ionicity of one, work well for most alkali halides, including LiF and NaF. The covalent-bond theory of Phillips and Van Vechten also predicts NaF should be highly ionic, possessing a fractional ionicity of 0.946, similar to other alkali halides.[27] On the other hand, there has been some indication from experiment that NaF may be different from other alkali halides,[21] and electron-diffraction investigations[28] have led to the conclusion that NaF is partially covalent. Analysis[29] of Compton scattering data is not conclusive, but seems to favor an ionic potential over a neutral-atom potential. These data need to be further examined to test the validity of approximations used[29] to describe the Compton scattering event.

†Work supported in part by the U. S. Air Force Office of Scientific Research under Grant No. AFOSR65-1565.

[1]F. Bloch, Z. Physik 52, 555 (1928).

[2]E. E. Lafon and C. C. Lin, Phys. Rev. 152, 579 (1966).

[3]R. C. Chaney, T. K. Tung, C. C. Lin, and E. E. Lafon, J. Chem. Phys. 52, 361 (1970).

[4]J. M. Tyler, T. E. Norwood, and J. L. Fry, Phys. Rev. B 1, 297 (1970).

[5]J. Callaway and J. L. Fry, in *Computational Methods of Band Theory*, edited by P. M. Marcus, J. F. Janak, and A. R. Williams (Plenum, New York, 1971), p. 512.

[6]R. C. Chaney, C. C. Lin, and E. E. Lafon, Phys. Rev. B 3, 459 (1971).

[7]J. M. Tyler and J. L. Fry, Phys. Rev. B 1, 4604 (1970).

[8]T. E. Norwood and J. L. Fry, Phys. Rev. B 2, 472 (1970).

[9]J. Callaway, H. M. Zhang, T. E. Norwood, and J. Langlinais, Int. J. Quantum Chem. 4, 425 (1971).

[10]J. Langlinais and J. Callaway, Phys. Rev. B 5, 124 (1972).

[11]J. L. Fry and D. M. Drost, Phys. Letters 35, 434 (1971).

[12]D. M. Drost and J. L. Fry, Phys. Rev. B 5, 684 (1972).

[13]R. N. Euwema and D. J. Stukel, Phys. Rev. B 1, 4692 (1970).
[14]For example, see L. J. Page and E. H. Hygh, Phys. Rev. 131, 3472 (1970); or A. B. Kunz, Phys. Rev. B 2, 5015 (1970).
[15]D. M. Roessler and W. C. Walker, J. Phys. Chem. Solids 28, 1507 (1967).
[16]K. E. Teegarden and D. B. Dutton, Phys. Rev. 155, 896 (1967).
[17]W. B. Fowler, Phys. Rev. 151, 657 (1966).
[18]R. C. Chaney, E. E. Lafon, and C. C. Lin, Phys. Rev. B 4, 2734 (1971).
[19]G. S. Painter, Int. J. Quantum Chem. (to be published).
[20]C. Gout, R. Frandon, and J. Sadaca, Phys. Letters 11, 656 (1969).
[21]S. W. Duckett and P. H. Metzger, Phys. Rev. 137, A953 (1965).
[22]R. Haensel, C. Kunz, T. Sasaki, and B. Sonntag, Phys. Rev. Letters 20, 1436 (1968).
[23]F. C. Brown, C. Gähwiller, H. Fujita, A. B. Kunz, W. Scheifley, and N. Carrera, Phys. Rev. B 2, 2126 (1970).
[24]For example, see D. M. Roessler and W. C. Walker, Phys. Rev. 166, 599 (1968); J. E. Eby, K. J. Teegarden, and D. B. Dutton, *ibid.* 116, 1099 (1959).
[25]C. Y. Fong and M. L. Cohen, Phys. Rev. Letters 21, 22 (1968); Phys. Rev. 185, 1168 (1969).
[26]C. Kittel, *Introduction to Solid State Physics* (Wiley, New York, 1971), p. 121.
[27]J. C. Phillips and J. A. Van Vechten, Phys. Rev. Letters 22, 705 (1969).
[28]A. G. Buntar and A. F. Margolina, Ukr. Fiz. Zh. 15, 359 (1970).
[29]T. Fukamachi and S. Hosoya, J. Phys. Soc. Japan 29, 736 (1970).

PHYSICAL REVIEW B VOLUME 6, NUMBER 10 15 NOVEMBER 1972

Effects of Domain Shapes on Second-Harmonic Scattering in Triglycine Sulfate

G. Dolino
Laboratoire de Spectrométrie Physique, Cédex 53 (38) *Grenoble-Gare, France*
(Received 30 March 1972)

A general description is given of the second-harmonic scattering of light by domains in a ferroelectric crystal. In addition to the usual second-harmonic beam, one observes second-harmonic light in new directions. The angular pattern of scattered light depends upon domain shapes. Plane parallel or cylindrical domains give very different diffraction diagrams. An experimental observation of this phenomenon in triglycine sulfate is given, where the variation of the second-harmonic intensity is correlated to changes in the domain structure. The anisotropy of the domains's cross sections leads to an anisotropic diffraction pattern.

I. INTRODUCTION

The phenomenon of second-harmonic generation (SHG) of light is observed when an intense light beam interacts with a noncentrosymmetric material.[1] If this material is inhomogeneous, second-harmonic scattering (SHS) is produced. This was observed for the first time in NH_4Cl by Freund[2] and then in triglycine sulfate (TGS).[3,4] The origin of this effect can be easily understood by considering the spatial modulation of nonlinear polarization by the domain structure. The effect of domains on the intensity of SHG was first observed by Miller on ferroelectric crystals of $BaTiO_3$.[5]

We have previously described the angular pattern of SHS which is observed on TGS crystals.[4] Here we give new theoretical and experimental results of the effects of domain shapes on SHS. The discussion is centered on ferroelectric materials, but some results can also be applied to the case of twins.

Section II is a general theoretical discussion of SHS where the effects of surface and domains are separated. Perfect correlation in one direction (cylindrical domains) or in two directions (plane parallel domains) leads to the characteristic scattering pattern. Particular attention is paid to the asymptotic behavior of the intensity for large scattering angles. In Sec. III new experimental results obtained at room temperature on TGS are presented. After recalling the main nonlinear optical properties of TGS we study the variation of intensity as a function of the scattering vector $\Delta\vec{k}$, the effect of the anisotropy of domain cross sections, and give some information on the effects of thermal treatments on domain structure and on SHS.

II. THEORY

A. Ferroelectricity and SHG

When a light beam with an electric field $\vec{E}_\omega$ of frequency ω is propagating in a crystal, it produces a linear polarization $\vec{P}_\omega = \overleftrightarrow{\epsilon} \cdot \vec{E}_\omega$ and also a nonlinear polarization $\vec{P}_{2\omega} = (\overleftrightarrow{d} \cdot \vec{E}_\omega) \cdot \vec{E}_\omega$ which is observable if the light beam is intense enough.[1] $\overleftrightarrow{\epsilon}$ is the linear susceptibility tensor and $\overleftrightarrow{d}$ the nonlinear susceptibility tensor. SHG can occur only in noncentrosymmetric crystals, which is the case in ferroelectrics.

In the phenomenological theory of ferroelectricity